Supporting Information

Facile fabrication of an ultra-light lithium-carbon nanotube thin film for precise prelithiation in lithium-ion batteries

Chao Wang, Fangzhou Yang, Wang Wan, Shihe Wang, Yongyi Zhang*, Yunhui Huang*, Ju Li**

1. Calculation of the energy density improvement and anode specific capacity

To calculate the relationship between specific capacity and energy density improvement for LFP||Gr pack level, we start by assuming a typical energy density of 160 Wh/kg for an LFP||Gr pack, and a specific capacity of 340 Ah/kg for the graphite anode with a working voltage of 3.2 V. Using the formula W% = E/(VC), we can calculate the weight percentage of graphite as W% = 160/(3.2*340) = 14.7%. For a future high energy density LFP||Gr pack of 220 Wh/kg, the weight percentage of graphite would be 20.2%.

To investigate the relationship between anode specific capacity, initial Coulombic efficiency (ICE), and energy density improvement for LFP||Gr pack level, we will consider two weight percentages, 15%, and 20%, in our calculations. Assuming an anode specific capacity of 340 Ah/kg and an ICE of 90%, we can use the following equation to calculate the relationship between energy density improvement (y) and anode specific capacity (x) for each weight percentage while maintaining a fixed ICE of either 80% or 90%:

For AM 15 and ICE 90%, the equation is y = 100/(340*15/x+85)-1
For AM 20 and ICE 80%, the equation is y = 100/(340*20/x+80)*80%/90%-1

By using these equations, we can determine how changes in anode specific capacity and weight percentage of graphite impact the energy density improvement of an LFP||Gr pack while considering the impact of ICE.

2. Supporting figures

Figure S1. Photograph of the CNT film at meter scale.

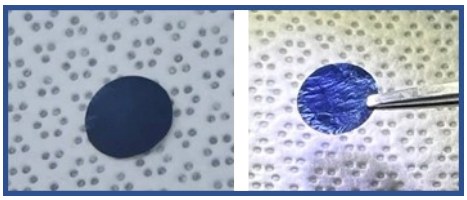

Figure S2. Photographs of the back of Li-CNT film

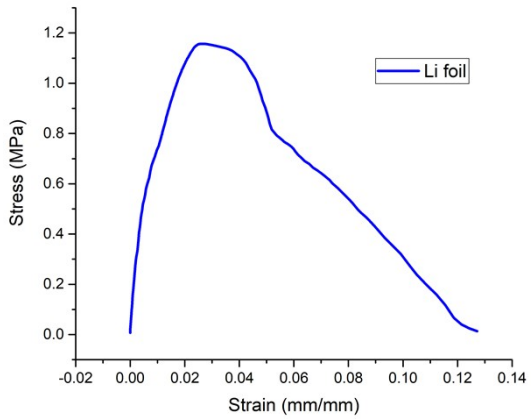

Figure S3. Tensile strength curve of pure lithium foil

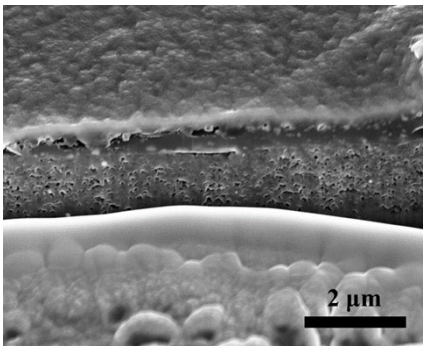

Figure S4. Cross-section images of the Li-CNT with a thickness of ~670 nm.

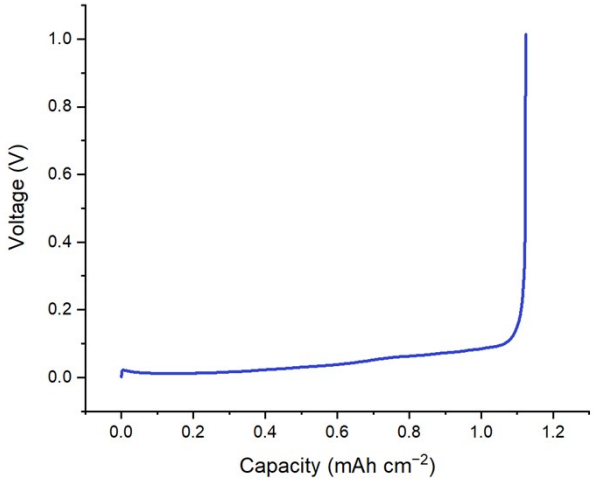

Figure S5. The stripping curve of Li-CNT with a capacity of around 1.12 mAh cm^{-2}

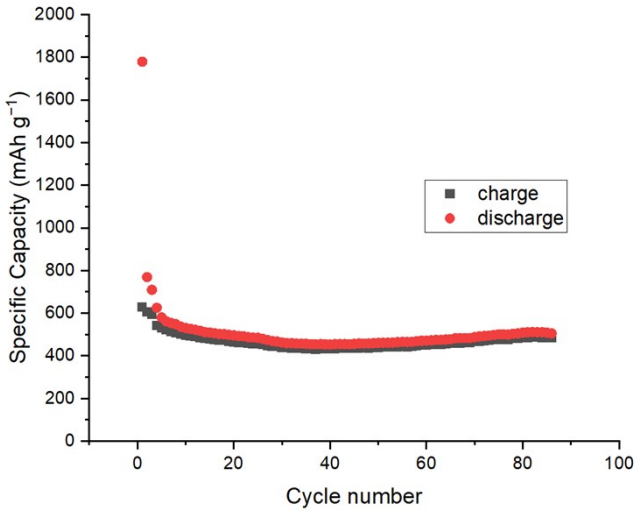

Figure S6. Cycling performance of the CNT film.

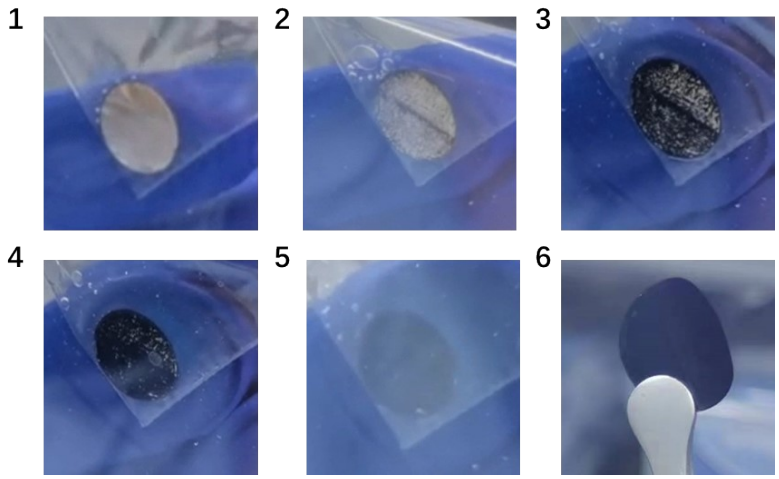

Figure S7. (1-5) Screenshots extracted from the Li-CNT film prelithiation process movie for the graphite electrode. (6) Image of the Li-CNT film with the side facing us after the prelithiation process.

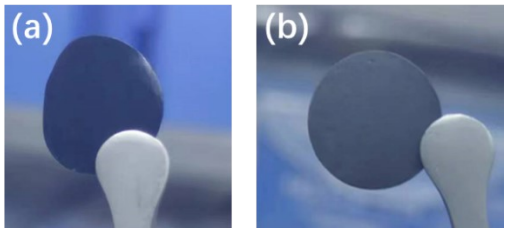

Figure S8. (a) Image of the Li-CNT film with the side facing the graphite electrode and (b) Graphite electrode after the in-situ prelithiation.

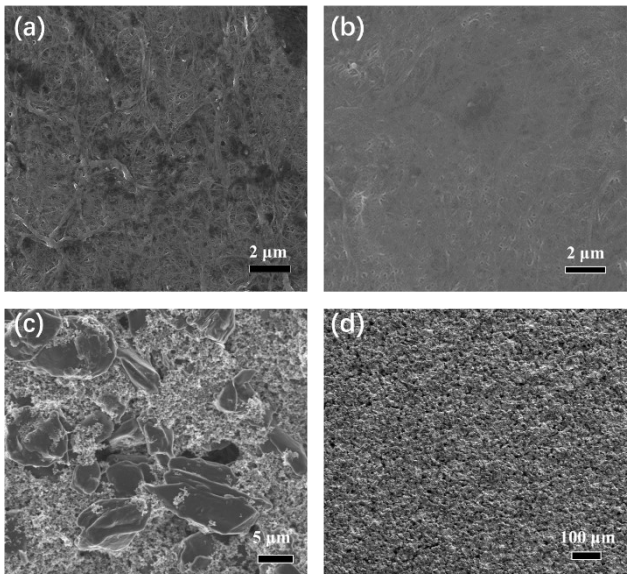

Figure S9. SEM images of the Li-CNT film after prelithiation in a coin cell: (a) the side face to graphite and (b) the opposite side. (c),(d) Graphite electrode after prelithiation.

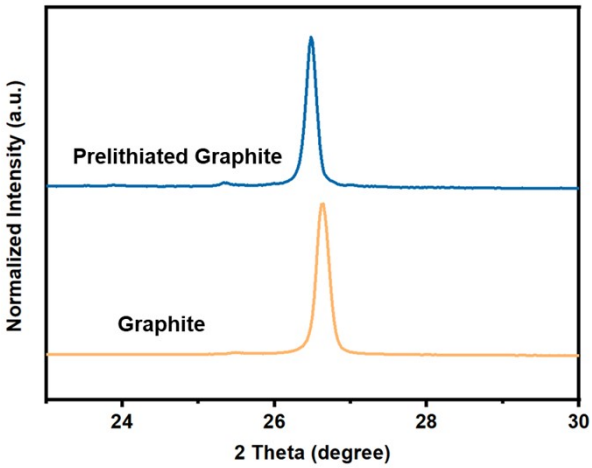

Figure S10. XRD of the graphite anode before and after Li-CNT prelithiation.

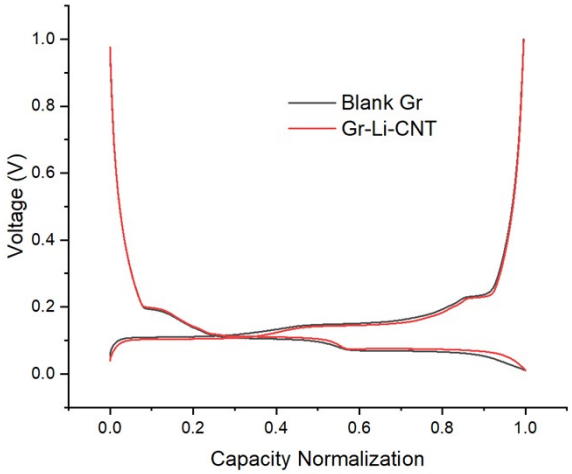

Figure S11. Charge and discharge curves of the blank and prelithiated graphite at the fifth cycle.

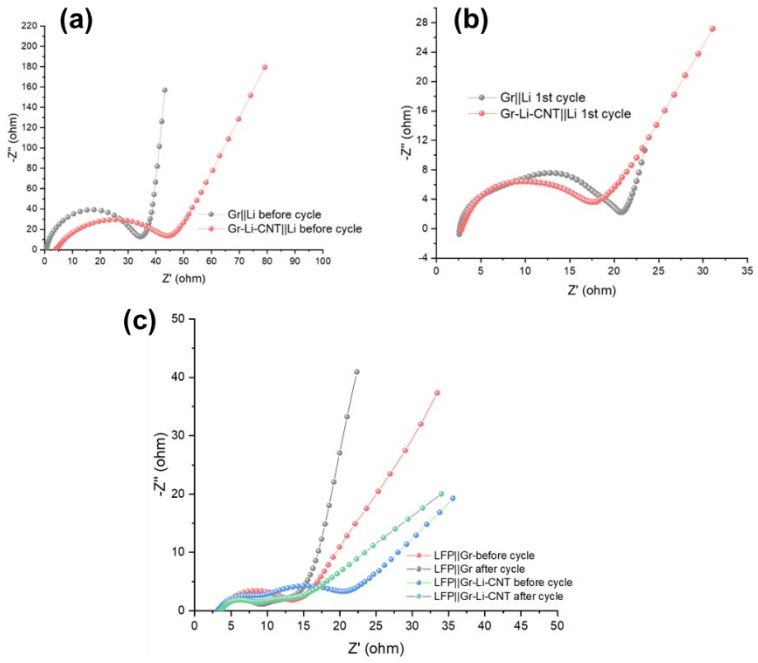

Figure S12. (a), (b) Impendence of graphite half cells with and without prelithiation, (c) LFP||Gr full cells with and without prelithiation.

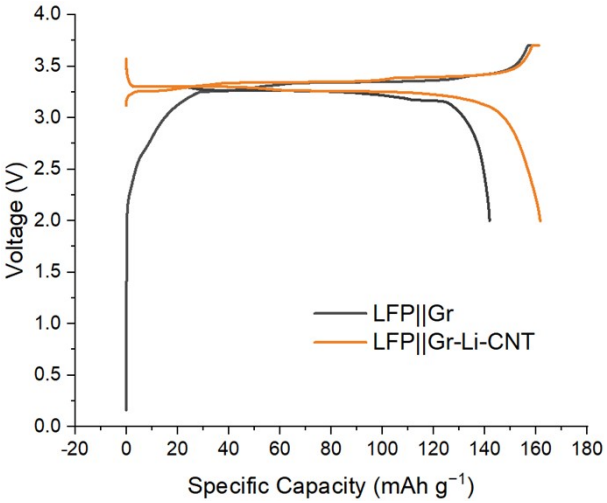

Figure S13. Charge and discharge curves of the initial cycle with Li-CNT prelithiation and without prelithiation when discharge to 2 V.

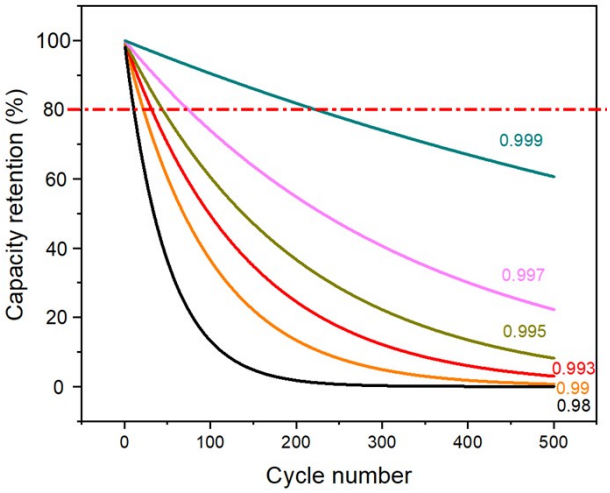

Figure S14. The relationship between cycle number and capacity retention

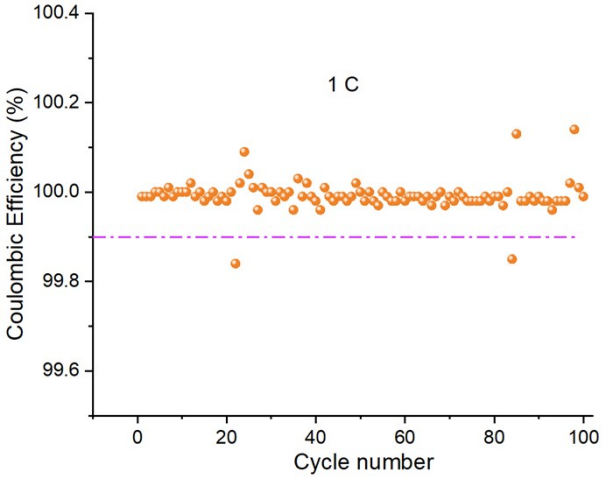

Figure S15. Coulombic efficiency of the LFP||Gr-Li-CNT full cell at 1 C.

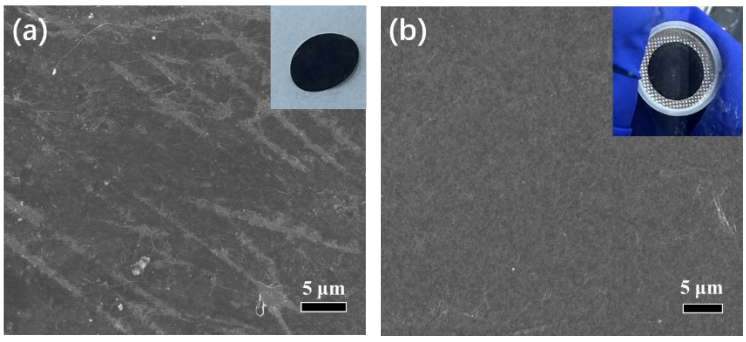

Figure S16. Photograph and SEM images of the Li-CNT film after (a) 50 cycles and (b) rate cycles.

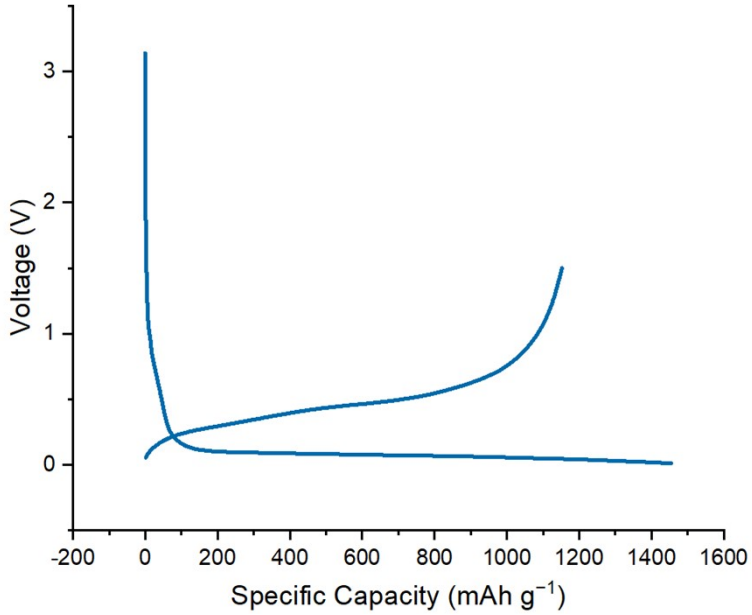

Figure S17. Initial charge and discharge profile of the silicon anode.

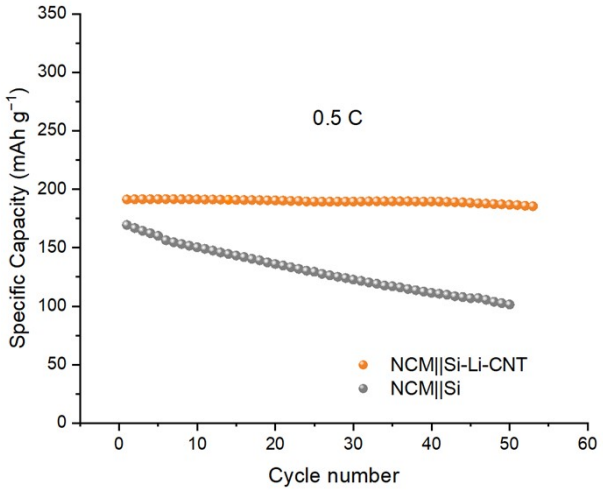

Figure S18. Cycling performance of NCM||Si and the prelithiatied NCM||Si-Li-CNT full cells at 0.5 C.

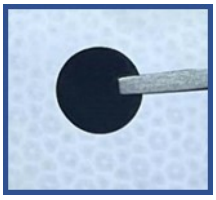

Figure S19. Additional photograph of Li-CNT film after lithium stripping

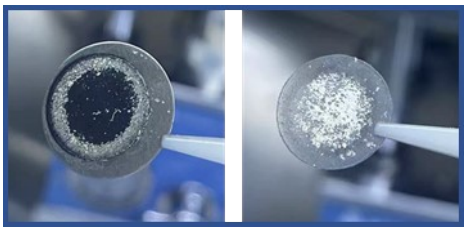

Figure S20. Photograph of the graphite anode after prelithation with lithium foil.